

## SiteFinder: A geospatial scoping tool to assist the siting of external water harvesting structures

R.G. Delaney, G.A. Blackburn, J.D. Whyatt, A.M. Folkard\*

Lancaster Environment Centre, Lancaster University, Lancaster LA1 4YQ, UK

### ARTICLE INFO

Handling Editor - Dr Z Xiyang

#### Keywords:

Water harvesting  
GIS  
Digital elevation model  
Remote sensing  
Drylands

### ABSTRACT

Water harvesting has a long history, but still plays an important role today by increasing crop productivity, combatting erosion, and improving water supplies. Geographical Information Systems (GIS) are used extensively to assess the suitability of sites for water harvesting but available tools fail to consider the synoptic topography of sites. Here, we report the creation of a novel, automated tool – “SiteFinder” – that evaluates potential locations by automatically calculating site-specific information, including structure parameters (height, length, and volume) and descriptors of the zone affected by the structure (storage capacity and area of influence) and the catchment area. Innovatively, compared to existing tools of this kind, SiteFinder works within a GIS environment. Thus, it allows the possibility of combining its outputs with larger Multi-Criteria Decision-Making processes to consider other bio-physical, socio-economic, and environmental factors. It utilises a Digital Elevation Model (DEM) and automatically analyses thousands of potential sites, computing site characteristics for different barrier heights that are dependent on the surrounding topography. It outputs values of eight parameters to aid planners in assessing the characteristics of sites as to their suitability for water harvesting. We conducted case studies using  $30 \times 30$  m gridded DEMs to automatically evaluate several thousand sites and, by filtering the tool outputs, successfully identified sites with characteristics appropriate for scenarios at three spatial scales: large dams for nationally significant water supply reservoirs (383 sites analysed; 5 filtered sites with barriers up to 30 m in height); large gully erosion control dams for regional-scale interventions (4,586 sites analysed; 6 filtered sites with barriers up to 3.6 m in height); and local, community-based earth embankment projects (801 sites analysed; 6 filtered sites with barriers up to 2 m in height). A higher resolution ( $1 \times 1$  m) terrain elevation model, derived from open-source airborne survey data, was used to assess the veracity of these results. Correlations between the barrier length, impounded area and storage volume capacity derived from the two different resolution data sets were all strongly significant (Spearman’s rank correlation,  $p < 0.001$ ); and normalised root mean square errors were 9%, 15% and 16% for these parameters, respectively.

### 1. Introduction

There is evidence that civilisations constructed water harvesting structures over four millennia ago (Critchley and Siegert, 1991), yet water harvesting continues to be widely used and the focus of ongoing research (Abdullah et al., 2020; Adham et al., 2019; Farswan et al., 2019; Haile and Suryabhagavan, 2019). It is practised primarily in arid and semi-arid regions (Bruins et al., 1986; Boers, 1994; Wang et al., 2008) where it is valuable as a way of bridging dry spells (Rockström and Falkenmark, 2015) and has been estimated to have the potential to increase crop production by up to 100% (Piemontese et al., 2020). Depending on the location and design, water harvesting structures can

serve different purposes, for example for the promotion of tree or crop cultivation (Mekdaschi and Liniger, 2013), artificial recharge of aquifers (Abdalla and Al-Rawahi, 2013; Şen et al., 2013), erosion control (Li et al., 2018), surface water storage (Sayl et al., 2019), or sub-surface water storage (Forzieri et al., 2008). Some form of water treatment (American Water Works Association, 2006; Logsdon, 2008; Siabi, 2008; Panagopoulos, 2021) will probably be required when harvested water is intended for domestic/industrial use, with the type of treatment dependent on the water quality problem (Cairncross and Feachem, 1993; Binnie et al., 2018).

Water harvesting structures vary from small pits or soil bunds made using hand tools, to earth embankments over a kilometre in length built

\* Corresponding author.

E-mail address: [a.folkard@lancaster.ac.uk](mailto:a.folkard@lancaster.ac.uk) (A.M. Folkard).

<https://doi.org/10.1016/j.agwat.2022.107836>

Received 6 April 2022; Received in revised form 13 July 2022; Accepted 14 July 2022

Available online 31 July 2022

0378-3774/Crown Copyright © 2022 Published by Elsevier B.V. This is an open access article under the CC BY license (<http://creativecommons.org/licenses/by/4.0/>).

with the aid of machinery. All water harvesting structures aim to reduce runoff and thus increase water storage. Depending on the technique implemented, water storage may take place in the soil; below the surface within introduced material such as sand; in surface water reservoirs; or in storage tanks. Water harvesting techniques are described as 'external' when they collect water originating from rainfall that has fallen elsewhere, while 'in-situ' water harvesting involves collecting rainfall on the surface where it falls (Helmreich and Horn, 2009).

Many previous studies have used Geographical Information Systems (GIS) to find potential locations for water harvesting structures without the need for field visits (e.g., Padmavathy et al., 1993; Al-Adamat, 2008; Ziadat et al., 2012; Kadam et al., 2012; Krois and Schulte, 2014; Al-Khuzaiet al., 2020). These methods invariably bring together different datasets, from remote sensing and digitised maps, often combined with hydrological modelling, and explore the decision-making space within the GIS environment.

When deciding if a location is appropriate for water harvesting there are numerous biophysical and socio-economic criteria to consider. In a review of 48 studies, Adham et al. (2016) identified nine biophysical criteria and nine socio-economic criteria that can be used to help assess the suitability of potential sites for water harvesting. Examples of biophysical criteria include rainfall (Tumbo et al., 2014), and drainage network metrics (Salih and Al-Tarif, 2012), while examples of socio-economic criteria include population density (Mati et al., 2006), and distance to crops (de Winnar et al., 2007). Adham et al. (2016) found that slope was the most common biophysical criterion used to identify water harvesting sites with 79% of all studies using slope as a criterion while only 55% of all studies used rainfall as a criterion. In all studies the slope data used is defined on a point-by-point basis, with flatter locations being identified as preferential for water harvesting locations. However, slope defined on a point-by-point basis does not consider the 'synoptic topography', or surrounding relief, which is crucial for identifying the potential of water harvesting locations. Moreover, while it may offer relevant information on the suitability of potential sites, it fails to provide the dimensions of necessary impounding structures (bunds or embankments) and the storage geometry they would create.

Automated tools working outside a GIS environment have been developed that consider the synoptic topography of potential sites and provide details of impounding structures and storage zones. For example, Petheram et al. (2017) created a novel set of algorithms to aid the siting of dams by providing dam and reservoir dimensions; Wimmer et al. (2019) introduced an automated method using contours to detect potential reservoir locations by calculating dam length and reservoir volume; and Teschemacher et al. (2020) describes an open-source MATLAB tool for determining dam and basin properties. Wang et al. (2021) reviewed dam siting methods and found that the majority were GIS-based, so it is argued that the siting tool introduced in this paper, which operates entirely within a GIS environment, will be of value to those involved in water harvesting site selection.

Open-source Digital Elevation Models (DEMs) are commonly used in selecting water harvesting sites. Typically, those used have a gridded resolution no finer than 30 m × 30 m. Higher resolution DEMs are available, but usually at significant, and in many cases prohibitive, cost. Schumann and Bates (2018) argued for freely available DEMs with global coverage, higher resolution and increased accuracy, as open source DEMs are poorly suited for many local-scale hydrologic applications. However, higher spatial resolution brings with it a problem for methods based on point-by-point defined variables in that the higher the resolution, the smaller each pixel becomes in relation to the land affected by a water harvesting structure. Thus, while there is an incentive to use higher resolution DEMs for enhanced hydrologic modelling this reduces the appropriateness of methods that rely on parameters defined on a point-by-point basis, such as the slope variable identified by Adham et al. (2016), that have been widely used hitherto.

The aim of the present study has been to provide a bridge between

the point-based slope criteria calculated in a GIS environment adopted by many researchers for water harvesting site selection and the automated methods that consider the surrounding topography of potential sites but work outside a GIS environment (Petheram et al., 2017; Wimmer et al., 2019; Teschemacher et al., 2020). This was approached by creating a GIS tool – "SiteFinder" – that can aid the siting of water harvesting structures by considering the synoptic topography of potential sites. The intended output of this approach is information about the length and height of potential impounding structures (barriers, hereinafter), and details of the areas of water storage they could create upstream of themselves. In essence, this is a similar approach to existing methods used to estimate the storage capacity of ponds (USDA, 1997) and small dams (Stephens, 2010) in so much as the area of water storage and the barrier height are used to compute predicted storage volume. The tool was designed to calculate the catchment area of each water harvesting structure since there is a correlation between catchment area and runoff efficiency (Karnieli et al., 1988; Boers and Ben-Asher, 1982), and the catchment area to cultivation area ratio is important for water harvesting sites designed for crop production (Critchley and Siegert, 1991). Finally, the tool was developed such that for every location analysed as a potential site for water harvesting, several barrier heights could be considered, up to a user-defined maximum height.

In summary the aim was to create an automated process capable of providing information on barrier size and water storage volumes for potential water harvesting sites that is not at present readily available within the convenient and widely used context of a GIS environment. The intention is that this could assist with scoping out potential sites, with an accuracy sufficient for the pre-feasibility stage of a project cycle. It is envisaged that this would need to be used alongside other biophysical, socio-economic and environmental information as part of decision-making processes.

## 2. Materials and methods

### 2.1. Tool development

The basic premise of SiteFinder is to take a basin elevation model and for each site of interest, compute the catchment area, create an imaginary axis perpendicular to the flow direction and perform analysis based on how the axis intersects with the model surface for varying heights above the elevation of the site. Tool outputs were compared against those derived manually using a dam site ground survey, and in addition, the tool was used to evaluate thousands of sites and rank them based on relevant parameters. The starting point for the developed tool is a raster-based Digital Elevation Model (DEM), which provides the primary source of elevation data. Clearly, the capability of the tool is in part dependent on the quality and resolution of the DEM used. This is considered further below, but it is described here with reference to a generic DEM, of no specific quality or resolution. SiteFinder is enacted using an ArcPy script within ArcGIS Pro. Through a series of steps, described below, it processes the DEM and creates outputs comprising information on the barrier (length, height, location, and orientation), the storage area the barrier would create, and the volume of the storage created.

Firstly, since the DEM may contain imperfections, a fill tool is used to remove any 'sinks' (spurious regions of lower elevation). The next step creates a flow direction raster (Fig. 1, "flow direction") using the 'filled' DEM as the input. Flow direction is defined as the direction from each cell to the steepest downslope neighbouring cell. The flow direction raster is then used to produce a flow accumulation raster (Fig. 1, "flow accumulation"), where flow accumulation is defined as the number of cells that flow into each downstream cell. Subsequently, only cells in the flow accumulation raster with values that fall within a range defined by the user prior to running the tool (based on the minimum and maximum catchment areas) are kept, while other cells are set to 'no data'. The amended flow accumulation raster, which effectively represents a

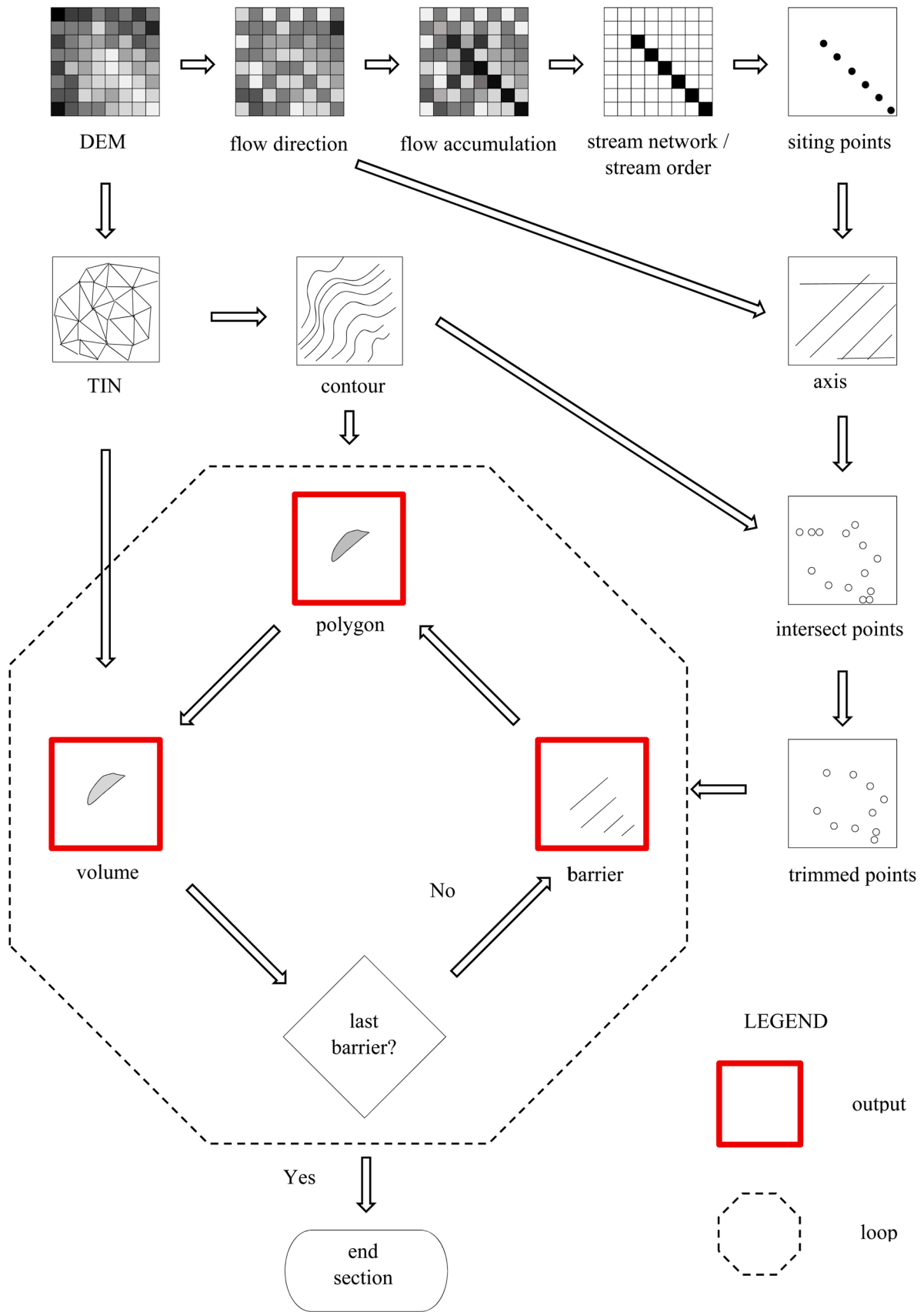


Fig. 1. Overview explaining how a DEM is used to obtain script outputs of polygons and volumes.

stream network, is then used, together with the flow direction raster, to create a stream order raster (Fig. 1, “stream network / stream order”), which classifies each cell using Strahler stream ordering, whereby the uppermost, headwater channels in a network are denoted first order, second order streams are those that result from the confluence of two or more first order streams; third order streams are those that result from the confluence of two or more second order streams, and so on, such that the largest, trunk channels in a network have the highest order (Strahler, 1957). The next step is to create siting points (Fig. 1, “siting points”) by creating a point located at the centre of every cell in the stream order raster. By default, all cells in the stream order raster become siting points but it is possible for the user to control which stream order cells become siting points.

Barrier information is then calculated and added to the siting points database. At every siting point, the SiteFinder script will, if the topography allows, create three barriers at different elevations, labelled A, B and C in order of increasing elevation. The user-defined maximum barrier height is used to calculate the barrier elevations. First, the maximum height is divided by three and the result converted to an integer. This integer is the step change in elevation between each barrier. Barrier elevations are then calculated by rounding up the DEM elevation at the siting point and adding the step change. For example, if the user enters a maximum barrier height of 10 m and the elevation at the siting point is 576.9 m then the first barrier (Contour A) elevation will be 580 m ( $577 + 3$ ), the second barrier (Contour B) elevation will be 583 m ( $577 + 6$ ) and third barrier (Contour C) elevation will be 586 m ( $577 + 9$ ).

The barrier axes pass through the siting point, with their direction set perpendicular to the siting point cell’s flow direction and their length equal to half the (user-defined) maximum barrier length on each side of the siting point (Fig. 2).

To determine the length of the top of each barrier, and subsequently the area of water they could impound, the points at which the barrier meets the ground needs to be determined. This requires putting the barrier axis direction into the context of the ground’s topographic contours. To achieve this, the DEM is used to create a Triangulated Irregular Network (TIN) (Fig. 1, “TIN”) elevation surface, from which a surface contour (Fig. 1, “contour”) shapefile is derived. The points at

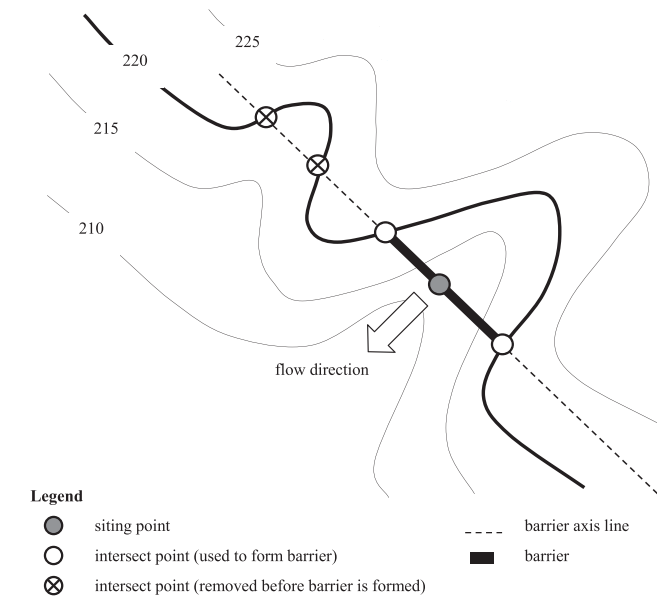


Fig. 2. Schematic showing the principal components of barrier creation, ●: siting point; ○: intersect point (used to form barrier), - - -; barrier axis line; █: barrier, ⊗: intersect point (removed before barrier is formed).

which the top of each barrier intersects the ground are then determined by intersecting the axis shapefile with the contour shapefile, producing intersect points (Fig. 1, “intersect points”) that are taken as the start and end points of the barrier. Each intersect point is linked with its associated siting point and barrier elevation (A, B or C) by a ‘contour label - siting point’ reference that is added to the intersect points database. Creation of barrier lines then requires locating two intersect points with identical ‘contour label - siting point’ references on either side of a given siting point (Fig. 2).

The first of several scenarios that may be encountered in this process is that there is no intersect point created for a siting point at an elevation corresponding to any of the barriers A, B or C. This will occur if the land is too flat and the top of the proposed barrier would not meet the surrounding land within half of the user-defined maximum barrier length from the siting point. The second scenario is that an intersect point is unique in that there is no other intersect point with the same ‘contour label - siting point’ reference. This case corresponds to the situation where the barrier top meets the ground as the latter rises up on one side of the siting point, but the land is too flat, or descending, for this to happen within the maximum barrier length on the other side. If either of these two scenarios occur, the site is rejected. The third scenario is that exactly two intersect points with the same ‘contour label - siting point’ reference are found, one on each side of the siting point and the site is identified as a potential water harvesting site. The final scenario is that more than two intersect points exist each having the same ‘contour label - siting point’ reference. In these final cases, SiteFinder identifies multiple intersect points (with identical ‘contour label - siting point’ references) on the same side of the siting point and deletes the more distant ones. The remaining intersect points are referred to as ‘trimmed points’ (Fig. 1, “trimmed points”), and these sites are also thus identified as potential water harvesting sites.

The next step is to create a line representing the top of each barrier. This is done using a points-to-line tool, which uses the ‘contour label - siting point’ references to create a straight line running from one intersect point, through the siting point to the corresponding intersect point on the other side. If for any siting point there is no intersect point or just a single intersect point at an elevation corresponding to A, B, or C then no barrier is formed since to create a line requires two identical ‘contour label - siting point’ references. Since any more distant intersect points have been deleted, barrier lines can only be formed using the two trimmed intersect points, one on either side of each siting point. These lines are stored as barrier shapefiles (Fig. 1, “barrier”).

Once the barrier lines have been created, SiteFinder then begins a loop, processing one barrier at a time. A polygon (Fig. 1, “polygon”) shapefile, representing the area of water storage that each barrier would impound, is created by combining the barrier line with a contour line that has the same contour identification reference as held in the barrier attribute field. This polygon is intersected with the TIN surface (Fig. 1, “TIN”) to obtain the volume (Fig. 1, “volume”) impounded by each barrier. For this to work, each polygon is assigned an elevation value set to the elevation of the top of the barrier with which it is associated.

The loop process ends once every barrier has been analysed. The polygons are then checked for artefacts created by closed contour lines, which result in more than one polygon per barrier. Artefacts are removed by calculating the distance of each polygon centroid to the barrier and removing all polygons except the nearest. The barrier shapefile is updated with the correct storage area and volume, and secondary raster information from the polygon feature class. Each row in the barrier feature class represents a unique barrier and is linked to a unique polygon by a barrier reference.

An estimation of the height of each water harvesting structure is carried out by taking the elevation of the barrier and subtracting the lowest elevation under the barrier profile on the TIN surface. In a similar manner the flow accumulation for each structure is found by extracting the maximum flow accumulation value along the barrier line. Elementary information contained within the barrier feature class is used to

calculate additional parameters (for example, catchment area to storage volume ratio) useful for water harvesting site selection. Eq. 1 is used to calculate the barrier volume (i.e., the volume of material that makes up the barrier) based on the geometry of a small earth dam (Nissen-Petersen, 2006), where  $V$  is the barrier volume ( $m^3$ );  $H$  is the maximum height (m) of the barrier before settling;  $L$  is the length (m) of the barrier crest;  $C$  is the width (m) of the crest; and  $S$  is the sum of the upstream and downstream slope. To simplify the comparison of results the crest width was fixed at 0.25 m and the sum of upstream and downstream slopes fixed at 5.5 for all case study scenarios.

$$V = 0.216HL(2C + HS) \tag{1}$$

### 2.2. Geometric validation of SiteFinder

To check that the fundamental geometrical aspects of the process

described above were functioning as intended, results produced by SiteFinder from a Shuttle Radar Topographic Mission (SRTM) void-filled, 3 arc-seconds (approximately 92 m grid resolution) DEM of an area in Sudan (Fig. 3a) were compared against results obtained manually using elevation data from an in-situ Differential Geospatial Positioning System (DGPS) dam site survey (Mohammed, 2018). The SRTM elevation data (Earth Resources Observation and Science (EROS) Center, 2018b) was selected as it is open-access, and the scale of the existing dam is far greater than a single 3 arc-second grid cell. The site is characterised by low-to-medium relief and SRTM products are considered to have small vertical errors in such circumstances (Falorni et al., 2005).

Before starting the processing, a comparison of elevations between the SRTM data (Fig. 3b) and the DGPS survey points was undertaken to establish the presence of any systematic vertical offset. A plot of SRTM elevation against the corresponding elevation from the DGPS survey (SM1, Supplementary Material) confirmed the presence of such an

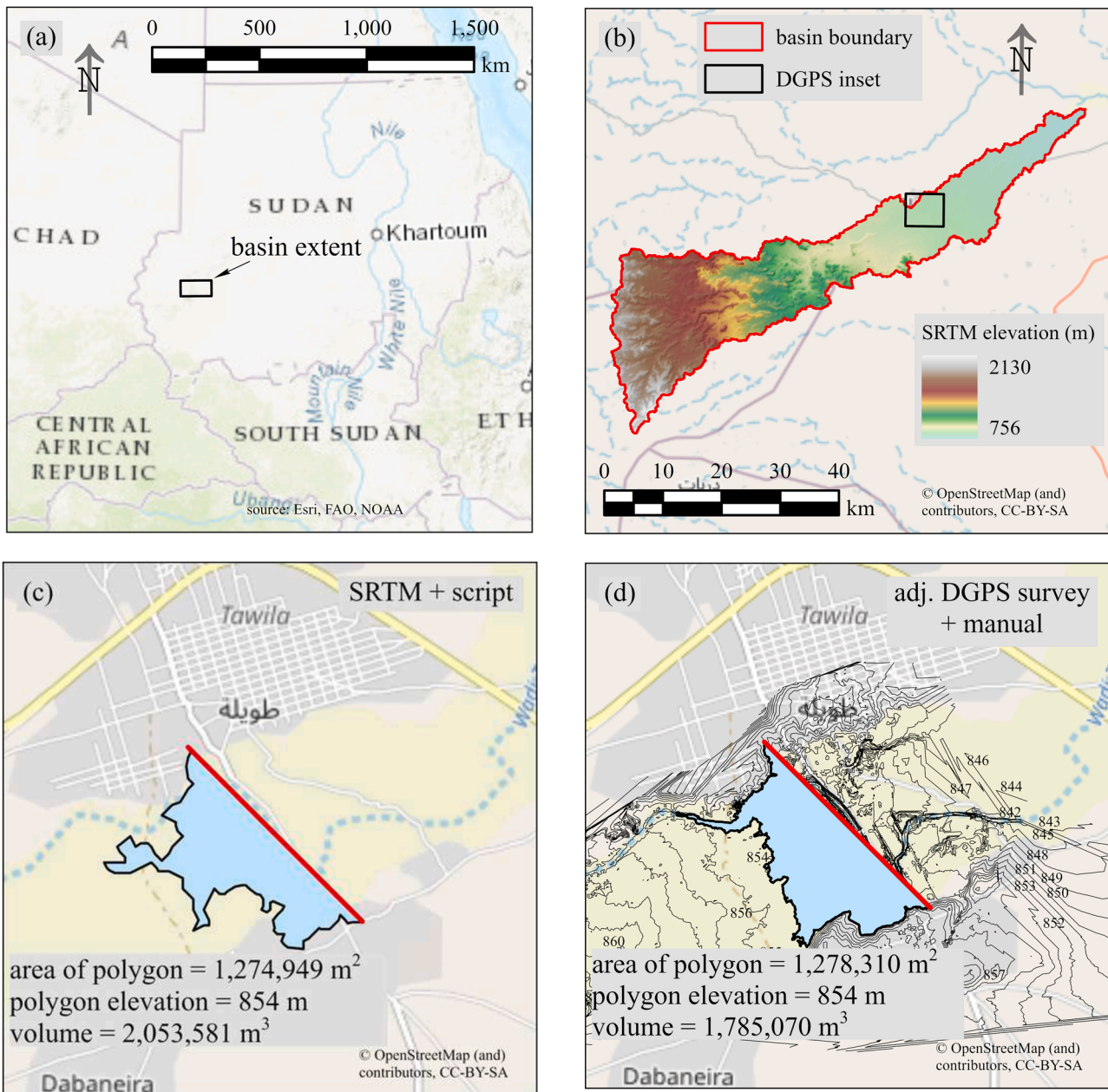


Fig. 3. Validation of the geometrical process: (a) country map with inset of basin extent, (b) Shuttle Radar Topography Mission (SRTM) 3 arc-second elevation of basin, (c) script outputs of barrier at 854 m based on SRTM DSM input, (d) barrier and polygon created manually using Differential Global Positioning System (DGPS) ground survey.

offset. The linear regression formula derived from this plot was applied to all DGPS points. The reduced vertical offset produced by this adjustment of the DGPS data can be observed by comparing the SRTM and adjusted DGPS contour lines (SM2, Supplementary Material).

A check was carried out to verify that the SiteFinder script was producing realistic measurements, for the polygon (area of influence) and volume (storage capacity). This was done by first selecting a barrier along with its associated polygon created by the script with the SRTM input (Fig. 3c) located within the boundary of the DGPS survey. A comparator barrier (and its associated polygon) was then created (Fig. 3d) manually by forming a barrier at the same elevation and orientation as the SRTM-derived barrier and intersecting it with the adjusted DGPS contours. The storage volume that would be impounded by these two barriers were calculated. The SRTM/SiteFinder method gave a polygon area of 1,274,949 m<sup>2</sup> and a storage volume of 2,053,581 m<sup>3</sup>, and the corresponding DGPS/manual process values were 1,278,310 m<sup>2</sup> and 1,785,070 m<sup>3</sup> respectively. This is a less than 1% difference for area and an approximately 15% difference for volume. In terms of area, at least, this difference demonstrates a strong level of consistency between the SRTM and DGPS-derived results. The 15% difference encountered when comparing the volumes may be explained by several factors including the period of 18 years between the SRTM and DGPS data acquisition. The SRTM survey is a Digital Surface Model (Gallant et al., 2012) which may have picked up the top of any vegetation or buildings rather than the ground, while the elevation points for the DGPS survey are of the dam structure and the ground surrounding the embankment only. Finally, the distance between the survey points for the DGPS ranged between 10 and 20 m and thus were better suited to capture relief features of the site compared to the 3 arc-seconds SRTM elevation product which resulted in a grid size of 92 × 92 m.

### 2.3. Application and validation to water harvesting scenarios

To assess its performance in a previously unexamined context, SiteFinder was applied to a different study area with the intention of identifying locations within it that have favourable characteristics for siting water harvesting structures. Three scenarios were explored, each one defined by constraints on the input parameters that resulted in a different scale of water harvesting structure being identified.

The study area used for this application is in central Ethiopia between latitudes 8.155–8.206 N and longitudes 38.937 E to 39.046 E. It covers an area of 68.4 km<sup>2</sup> (12 km × 5.7 km) and has an elevation range of slightly over 600 m (Fig. 4) and is representative of the arid to semi-arid regions where water harvesting techniques are most commonly implemented. The digital elevation data to which the process was

applied was taken from the 1-arc second global digital elevation product from the NASA Space Shuttle Radar Topography Mission (SRTM), which is freely available via the US Geological Survey (Earth Resources Observation and Science (EROS) Center, 2018a). This is a digital surface model (DSM) rather than a digital terrain model (DTM) but offers good coverage of arid and semi-arid regions and is often used for water harvesting site selection (Vema et al., 2019; Mugo and Odera, 2019).

In Scenario 1, the rationale was to imitate a national governmental department tasked with finding sites suitable for large dams with the primary purpose of creating water supply reservoirs. Candidate sites were sought that would be able to accommodate structures with a barrier height of over 15 m – to meet a definition of a large dam (ICOLD/CIGB, 2011) but not greater than 25 m. Other defined criteria included storage capacity in excess of 1,000,000 m<sup>3</sup> and a storage volume to barrier volume ratio of at least ten, the latter acting as an indicator of value-for-money. Finally, the dam length was constrained to be no greater than 2,000 m. The minimum and maximum catchment areas were set to 2,000,000 m<sup>2</sup> and 9,000,000 m<sup>2</sup> respectively following analysis of a flow accumulation raster to identify the most significant drainage channels within the AOI. The search parameters are summarised in Table 2.

Scenario 2 aimed to replicate the implementation of a water harvesting techniques at a scale of interest to planners at a regional level. SiteFinder was therefore used to search for sites suitable for large gully erosion control check dams, classified when the gully depth is more than 5 m (Geyik, 1986). The search parameters are summarised in Table 3.

Scenario 3 was intended to resemble a community-based project, possibly supported by a non-governmental organisation, whose goal is to increase crop productivity by placing more agricultural land under flood. The water harvesting structure considered therefore is in the form of earth embankment, no more than 2 m in height, intended to hold back runoff, and as the dry season advances water loss through evaporation causes more land to become available for planting, similar to some earth embankment dams in Sudan (Zumrawi, 2015) and comparable in purpose to the traditional *Teras* system (Van Dijk and Ahmed, 1993; Nijmeijer, 1998) also found in Sudan. In this scenario embankments should be no more 400 m in length. Since the aim of project is to bring land under irrigation the desired feature of any site is the area of influence (the saturated zone upstream of the barrier) which should be a minimum of 10,000 m<sup>2</sup>. To identify locations that offer acceptable value-for-money barriers would only be considered viable if the area of influence to barrier volume ratio is equal or greater than one hundred. The search parameters are summarised in Table 4.

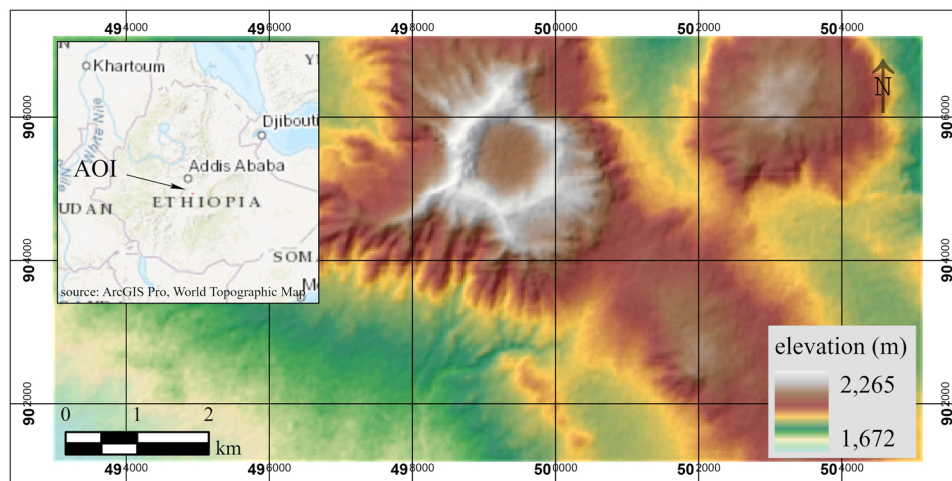


Fig. 4. Ethiopia: area of interest (AOI) showing Shuttle Radar Topography Mission (SRTM) elevation data with country level map (inset).

## 2.4. High-resolution DEM

To test the accuracy of the process using the 1 arc-second resolution DSM, it was repeated for each of the three scenarios using a higher resolution DEM and the results compared. The higher resolution DEM was found using an open topography website ([OpenTopography, 2008](#)) and consisted of a 1 m × 1 m resolution product obtained using a LiDAR instrument by the UK Natural Environment Research Council Airborne Research and Survey Facility ([Airborne Research and Survey Facility, 2009](#)).

The comparison of results from the two elevation data products was carried out using a modified version of SiteFinder, so that while the siting points and axis directions were derived from the SRTM DSM the actual barriers and storage volumes were created on a LiDAR DTM elevation surface. This approach allowed a comparison of barriers and impoundments to be made for barriers formed at the same location, in the same direction and of a similar height, but using elevation models of different resolutions, thereby isolating the effects of the resolution change.

From the matching pairs of barrier data, three parameters were analysed to assess the comparison of the SRTM-based results and the LiDAR-based results. Barrier length, area of influence and storage volume were chosen since these metrics play a significant role in the water harvesting site selection, either directly or indirectly, and they cover dimensions of length, area, and volume. Comparisons of these parameters from the two elevation data products were carried out using Spearman's rank correlation tests and Root Mean Square Error (RMSE) analysis.

## 3. Results

### 3.1. High-resolution DEM

The modified version of SiteFinder identified 903 barriers in the LiDAR DTM. These were compared against barriers identified in the SRTM DSM. However, since there is a difference between the two elevation models not all barriers (with a shared siting point and contour reference) formed on the LiDAR DTM model were also formed on the SRTM DSM surface. Barriers sharing the same siting point, the same contour reference and formed on both elevation models were matched. The results of the statistical comparisons of parameters derived from each DEM are presented in [Table 1](#). Charts of each metric are provided in [Supplementary Materials](#).

### 3.2. Scenario 1 case study - large dam

The results for Scenario 1 are presented in [Table 2](#). In total, SiteFinder identified 383 siting points and created 376 barriers. The initial desired minimum storage volume was set at  $1 \times 10^6 \text{ m}^3$  while SiteFinder outputted barriers with a maximum storage volume  $13.9 \times 10^6 \text{ m}^3$  and

**Table 1**

Analysis of results from all case study scenarios comparing barrier length (L), polygon area (A), and storage volume (V) using Shuttle Radar Topography Mission (SRTM) elevation data against high-resolution Airborne Research and Survey Facility LiDAR data.

		$L_{\text{SRTM}}$ $L_{\text{LiDAR}}$	$A_{\text{SRTM}}$ $A_{\text{LiDAR}}$	$V_{\text{SRTM}}$ $V_{\text{LiDAR}}$
Spearman's rho	Correlation Coefficient	.568 **	.683 **	.721 **
	Sig. (1-tailed)	< 0.001	< 0.001	< 0.001
	N	685	685	685
Root Mean Square Error		188 m	78,887 m <sup>2</sup>	552,018 m <sup>3</sup>
Normalised Root Mean Square Error (RMSE divided by LiDAR mean)		0.91	1.15	1.16

\*\*Correlation is significant at the 0.01 level (1-tailed).

**Table 2**

Case study Scenario 1: desired parameters, search parameters, tool output parameters, filter limits and parameter range of filtered barriers.

scenario reference	Scenario 1					
implementation level	national					
structure type	large dam					
primary purpose	water supply					
parameter	limit	desired	search	output	filter	range
barrier height (m)	min.	15	10	10		20
	max.	25	30	30		23
barrier length (m)	min.			68		1004
	max.	2,000	2,000	1427		1,216
area of influence (10 <sup>6</sup> m <sup>2</sup> )	min.					1.0
	max.					1.2
catchment area (10 <sup>6</sup> m <sup>2</sup> )	min.		2			3.6
	max.		9			6.1
storage volume (10 <sup>6</sup> m <sup>3</sup> )	min.	1		0.1	10.0	6.1
	max.			13.9		13.9
storage to barrier volume ratio (-)	min.	10		0.0	10.0	15.4
	max.			33		23.9
catchment area to storage volume ratio (m <sup>-1</sup> )	min.					0.3
	max.					0.5
siting points (N <sup>2</sup> )				383		5
barriers (N <sup>2</sup> )				376		5

since storage volume was considered to be an important metric it was decided to increase the minimum storage volume, so a filter was applied resulting in only barriers with a storage volume equal or greater than  $10 \times 10^6 \text{ m}^3$  were included in the final barrier list.

The storage to barrier volume ratio (SBVR) for some barriers fell well below the desired ratio of ten, so these were removed by applying a filter, resulting in the filtered barriers having a SBVR not less than 15.4. Consequently, only five barriers remained. Although these were all associated with different siting points, those point were all clustered together, thus effectively, a single site was identified ([Fig. 5](#)).

The ranges of values of parameters defining the identified barriers and impoundments are shown in [Table 2](#). This information could be used to inform decisions as to whether it would be worthwhile investigating sites as potential water harvesting locations. In this scenario, planners would observe that the catchment area to storage volume ratio is no greater than  $0.5 \text{ m}^2 \text{ m}^{-3}$  for any of the identified barrier locations and may conclude this is insufficient to generate the inflows needed to fill the dam and hence decide not to pursue the site as a location for a large dam. For comparison, [Papenfus \(2003\)](#) describes three potential dams with catchment area to storage volume ratio ranging from 69 to  $122 \text{ m}^2 \text{ m}^{-3}$ , drought reserve dams should have a catchment area to storage volume ratio from 50 to  $100 \text{ m}^2 \text{ m}^{-3}$  ([Agriculture Victoria, 2020](#)) and [Nissen-Petersen \(2006\)](#) details a dam design with a catchment area to water storage volume of  $333 \text{ m}^2 \text{ m}^{-3}$ .

### 3.3. Scenario 2 case study - gully check dam

The results from Scenario 2 are presented in [Table 3](#). SiteFinder identified only 23 barriers from a total of 4586 siting points analysed. Of these, some had very low SBVRs. A filter was applied that removed all those with SBVR < 2.5, resulting in six barriers at different siting points across the study area, although two barriers are located in the same gully separated by only 30 m. While the filtered barriers met the desired parameter ranges for barrier length and catchment area, they all fell outside the desired range for the parameters of catchment area to storage volume ratio (< 15 m<sup>-1</sup>) and barrier height (5–7 m). From the results of the filtered barriers the ranges of storage volume, catchment area and barrier height were 900,000–2300,000 m<sup>3</sup>, 60,000–200,000 m<sup>2</sup>, and 3–3.6 m respectively. [Ettazarini \(2021\)](#) describes small check dams having a storage volume up to 500,000 m<sup>3</sup>, while [Geyik \(1986\)](#) defines medium sized gully dams having a

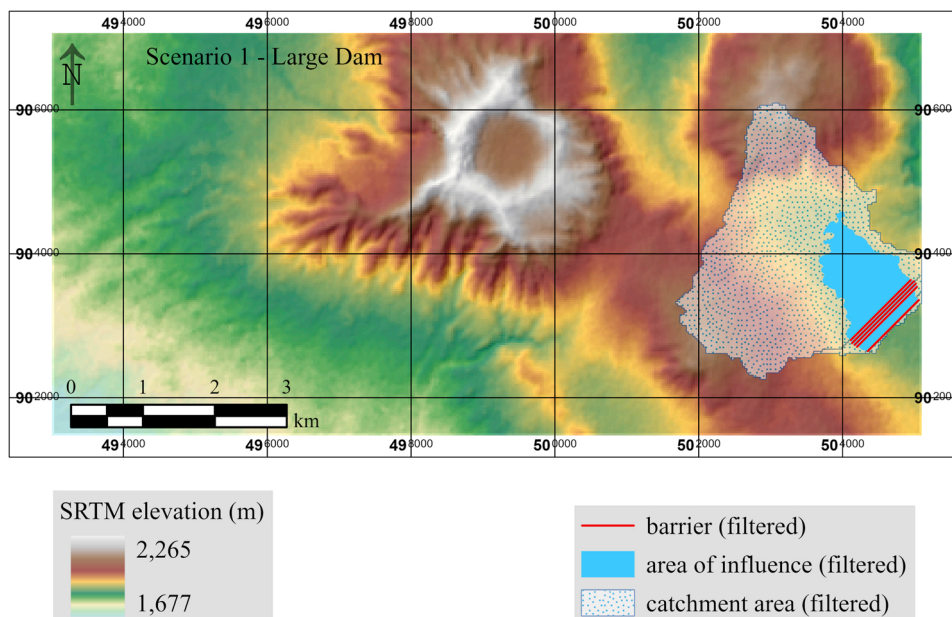


Fig. 5. Scenario 1 (Large Dam) results using Shuttle Radar Topography Mission (SRTM) elevation data.

**Table 3**  
Case study Scenario 2: desired parameters, search parameters, tool output parameters, filter limits and parameter range of filtered barriers.

scenario	Scenario 2					
reference						
implementation level	regional					
structure type	gully check dam					
primary purpose	erosion control					
parameter	limit	desired	search	output	filter	range
barrier height (m)	min.	5	3	3		3
	max.	7	9	6.5		3.6
barrier length (m)	min.			19		24
	max.	40	40	39		39
area of influence (10 <sup>6</sup> m <sup>2</sup> )	min.					0.7
	max.					1.6
catchment area (10 <sup>6</sup> m <sup>2</sup> )	min.	0.05	0.05	0.04		0.06
	max.	0.4	0.4	0.4		0.2
storage volume (10 <sup>6</sup> m <sup>3</sup> )	min.					0.9
	max.					2.3
storage to barrier volume ratio (-)	min.			0.4	2.5	2.8
	max.			7.8		7.8
catchment area to storage volume ratio (m <sup>-1</sup> )	min.	5		35		35
	max.	15		2,467		170
siting points (N <sup>⊙</sup> )				4,586		6
barriers (N <sup>⊙</sup> )				23		6

catchment area range of 20,000–200,000 m<sup>2</sup> and a range of gully depth of 1–5 m, so while the intention was to locate large gully check dams SiteFinder results appear to show that sites for medium sized check dams have been identified.

The six filtered barriers, located in a total of five gullies, together with the respective area of influence and catchment area of each barrier are shown in Fig. 6.

### 3.4. Scenario 3 case study - earth embankment

The results for Scenario 3 are presented in Table 4. In total 801 siting points were analysed as potential sites for earth embankments resulting in potential barriers.

A barrier height filter was applied so that all barriers would be at least 1 m and no greater than 2 m. Placing a maximum limit on the

height of filtered barriers of just 2 m increases the prospect that the construction could be accomplished using local oversight and labour as the work is technically less demanding than constructing higher embankments.

A high proportion (508 from a total 1,771) of outputted barriers had a SBVR ranging from zero to almost three, so a filter (equal or greater than 3) was applied to ensure these barriers were not included in the final list selected barriers.

In this scenario the purpose of the water harvesting structure is to provide irrigated land immediately upstream of the barrier (i.e., the area of influence) so a condition was applied to ensure that all filtered barriers provided at least 100 m<sup>2</sup> of irrigated land for every cubic metre of embankment constructed. This demonstrates the capacity of SiteFinder to output a ‘socio-economic’ criterion, since the area of influence to barrier volume ratio is an indicator of value-for-money.

A catchment area to storage volume ratio filter was applied that set an upper limit of 15 m<sup>-1</sup> as a way of controlling the amount of runoff a water harvesting site would receive. The rationale behind such a filter is that planners may wish to avoid sites where excess runoff might require expensive technical solutions and focus on sites where excess runoff is less problematic.

Of the seven barriers filtered from the initial 1,771 barriers the SBVR was found to range from 234 to 1,374 (Table 4). SiteFinder calculates the storage to include the volume of any natural depressions (i.e., pools) should they occur within the area of influence, together with storage created as a direct result of the barrier. SiteFinder is able to compute the volume of natural depressions as it computes site geometry based on a TIN surface (Fig. 1) created using a DEM that has not been ‘filled’ to remove ‘sinks’.

Table 4 shows the range of parameter values for both the total unfiltered 1,771 barriers and the seven filtered barriers. The final filtered barriers, all of which meet the ‘desired’ criteria (Table 4) are distributed in three distinct clusters (Fig. 7).

## 4. Discussion

The case studies demonstrate how SiteFinder can analyse automatically thousands of potential external water harvesting sites within a GIS environment and provide useful information (e.g., barrier volume and storage capacity) using a digital elevation raster as the primary data

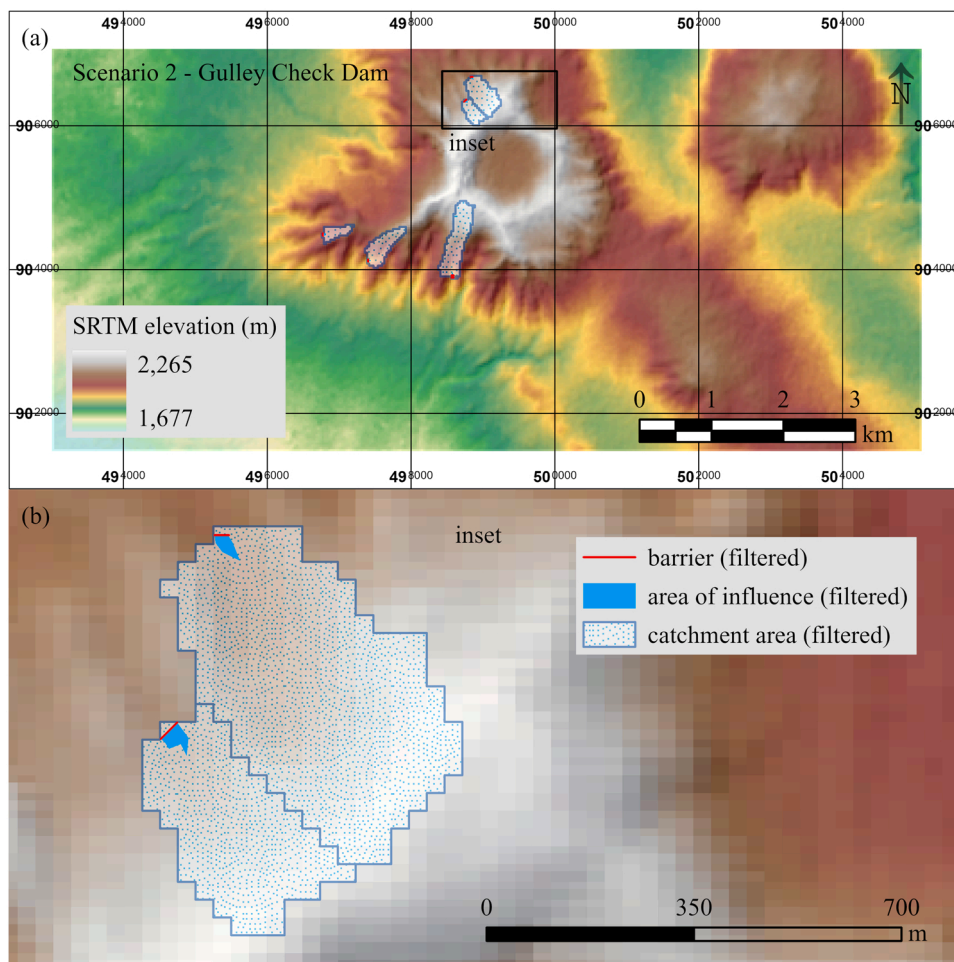


Fig. 6. (a) Scenario 2 (Gulley Check Dam) results using Shuttle Radar Topography Mission (SRTM) elevation data with inset box, (b) inset of two filtered barriers with their respective area of influence and catchment area.

Table 4

Case study Scenario 3: desired parameters, search parameters, tool output parameters, filter limits and parameter range of filtered barriers.

scenario reference	Scenario 3					
implementation level	community					
structure type	earth embankment dam					
primary purpose	irrigation (flood recession)					
parameter	limit	desired	search	output	filter	range
barrier height (m)	min.	1	0	0	1	1
	max.	2	3	8	2	2
barrier length (m)	min.		0	0.4		55
	max.	400	400	377		180
area of influence ( $10^6 \text{ m}^2$ )	min.	0.01				0.04
	max.					0.1
catchment area ( $10^6 \text{ m}^2$ )	min.	1	1	0.5		0.9
	max.	5	5	6.9		2.0
storage volume ( $10^6 \text{ m}^3$ )	min.					0.1
	max.					0.2
storage to barrier volume ratio (-)	min.			0	3	234
	max.			1,374		1,374
area of influence to barrier volume ratio ( $\text{m}^{-1}$ )	min.	100		0.2	100	114
	max.			837		717
catchment area to storage volume ratio ( $\text{m}^{-1}$ )	min.			4.7		8
	max.			$28 \times 10^9$	15	13
catchment area to cultivation area ratio (-)	min.			12		16
	max.			$112 \times 10^6$		33
siting points ( $\text{N}^2$ )				801		6
barriers ( $\text{N}^2$ )				1,771		7

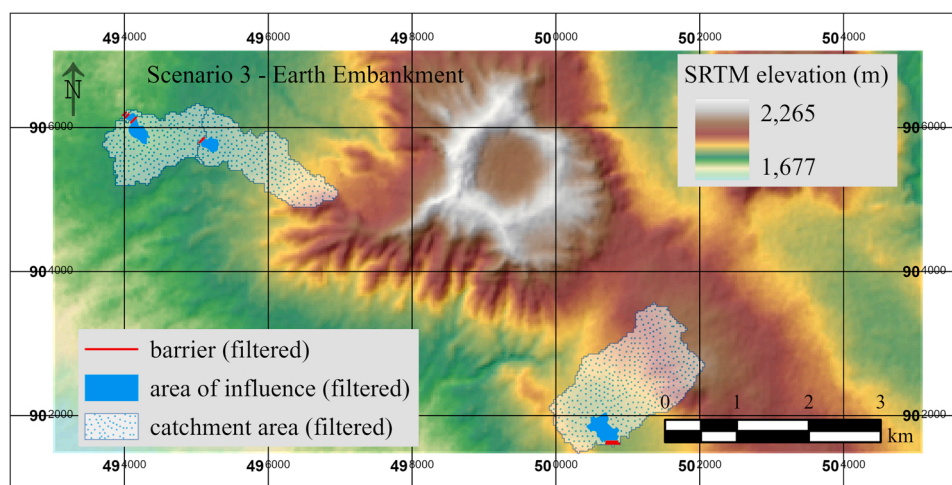


Fig. 7. Scenario 3 (Earth Embankment) results using Shuttle Radar Topography Mission (SRTM) elevation data.

source. The automated method runs entirely within the GIS environment and provides information for site selection purposes (e.g., barrier dimensions and storage geometry) which cannot be obtained from a slope raster, which is most the common type of dataset currently used by researchers for water harvesting site selection (Adham et al., 2016). Bespoke software and tools (Petheram et al., 2017; Wimmer et al., 2019; Teschemacher et al., 2020) do exist that automate the process of extracting dam details for potential sites but all function outside a GIS environment. DamSite (Petheram et al., 2017) is a bespoke software that uses algorithms and a pixel-based process to obtain dam site information but not provide polygons of the area of influence and cannot be applied to very small basins (Teschemacher et al., 2020). Wimmer et al. (2019) used a point cloud processing software OPALS with outputs stored in a GIS vector dataset but their results do not include details of barrier volume and catchment area. An open-source MATLAB tool developed by Teschemacher et al. (2020) requires the user to incorporate all criteria (e.g., settlement area) in order for sites with the best potential to be identified. The SiteFinder tool described here does not aim to provide the answer to where the best water harvesting sites are but rather provides relevant barrier characteristics, calculated within the GIS environment, allowing the possibility of readily incorporating results into a multi-criteria decision-making process, again using the GIS environment, which would allow the consideration of other biophysical, socio-economic, and environmental factors.

Integral to the functioning of SiteFinder is the use of flow direction to determine the orientation of the barrier (set perpendicular to flow direction), which is an innovative feature for an automated water harvesting site selection process. This has the benefit of allowing SiteFinder to scan a higher number of locations as processing time required to optimise barrier orientation is avoided. Unlike some site selection tools (Wimmer et al., 2019; Teschemacher et al., 2020) SiteFinder considers catchment area. Catchment area is related to runoff efficiency (Karnieli et al., 1988) and the volume of runoff a water harvesting site will receive. SiteFinder calculates catchment area and uses it to search for potential sites and outputs water harvesting site characteristics including catchment area to cultivation area (Critchley and Siegert, 1991). This implies that if data on annual catchment runoff were available, SiteFinder would readily be able to output the site selection criterion of inflow to storage volume ratio (Papenfus, 2003) using the catchment area to storage volume ratio that it already calculates.

Often the choice of which locations should be reviewed for potential water harvesting sites involves an amount of human interpretation of maps to judge the best spots or “narrows” (Forzieri et al., 2008) as places to be analysed for suitability. SiteFinder offers an objective and repeatable alternative to identify sites with favourable characteristics.

For the siting of large water harvesting structures there is an argument that human interpretation alone can identify sites of interest that warrant further analysis. For example, in Scenario 1 (Fig. 5) there are only a few places that a large dam could be sited, and these locations could possibly be ascertained using visual interpretation of maps alone. However, the same task becomes extraordinarily difficult for smaller water harvesting structures like those described in Scenario 2 (Fig. 6) and Scenario 3 (Fig. 7).

For a small dam the volume of material required to construct the barrier itself can represent approximately sixty percent of the Bill of Materials (Nissen-Petersen, 2006). The barrier volume therefore can be used as a proxy for capital cost. SiteFinder calculates the barrier volume based on the barrier length and barrier height. However, planners invariably want to establish the cost-benefit of any proposed scheme in the initial stages of the project cycle. To address this, SiteFinder provides the storage volume to barrier volume ratio and area of influence to barrier volume ratio (Table 2), either of which could aid a decision-making process on site suitability. Of the forty-eight papers reviewed by Adham et al. (2016) only four refer to cost. One uses a fixed cost for the water harvesting solution (Jothiprakash and Sathe, 2009), two use price-of-land (Banai-Kashani, 1989; Sekar and Randhir, 2007), and only one (Forzieri et al., 2008) considers the water storage volume against the volume of the dam (or barrier volume) but in a process that requires visual interpretation of satellite imagery to estimate the width of “narrows”. SiteFinder provides an automated process that bridges biophysical criteria (e.g., area of influence) with socio-economic criteria, e.g., cost-benefit information in the form of storage volume to barrier volume ratio.

SiteFinder calculates the barrier height based on the elevation profile along the entire barrier crest and similarly the catchment area of the site is based on flow accumulation associated with the barrier crest line. This method is therefore arguably more sophisticated than other site selection methods that establish site suitability using single raster cell values, e.g., slope. SiteFinder considers potential water harvesting sites in full, extracting and using values from any number of raster cells and so represents a shift away from a single cell approach to one whereby the water harvesting structure is considered as a complete entity. A problem with using values obtained at single raster cells to support a site suitability assessment is that as the cell size decreases (due to the use of a higher resolution dataset) the size of the raster cell becomes smaller in proportion to the water harvesting structure, although it is possible to calculate surface parameters (including slope) using windows greater than the normal default size of  $3 \times 3$  cells. Better elevation data, in terms of vertical accuracy and spatial resolution, is associated with regional and local scale data (Schumann and Bates, 2018) and since it

has been demonstrated that SiteFinder can be successfully used with high resolution datasets such as LiDAR (Table 1) it therefore can exploit the increased detail these DEMs offer in a way that techniques that assess site suitability based on values at individual raster cells cannot.

For every barrier created by SiteFinder a polygon is also created that represents the area of influence (saturated zone) upstream of the water harvesting structure. These polygons represent the area affected by the barrier in a more realistic way compared to representing a water harvesting structure by a single point (or raster cell) or just the barrier alone. As part of a site selection process these area of influence polygons could be overlaid with land use and land cover maps. For example, if the purpose of the water harvesting structure is to facilitate artificial groundwater recharge (Zaidi et al., 2015) the polygons defining the area of influence could be overlaid with soil texture and vadose zone thickness maps to enable the hydrological response to be more realistically assessed. Selection criteria have been presented in the case studies presented (Table 2, Table 3, Table 4) but SiteFinder outputs allow users to formulate other criteria that they may consider useful in a site selection process. For example, it may be useful to know the area of influence to storage volume ratio as a way of limiting evaporation (Reseigh, 2021) and this could simply be obtained since both parameters (area of influence and volume) are contained within the barrier database. As SiteFinder works within a GIS environment combining its results with other parameters is straightforward, requiring no additional software. For instance, the catchment area calculated by SiteFinder in case study Scenario 2 could be used together with the slope (calculated using GIS but not with SiteFinder) to ascertain the runoff energy which is strongly associated with erosion control check dam collapse (Castillo et al., 2007).

The case studies presented above utilised a 1 arc-second (30 m x 30 m) SRTM DSM. The resulting barriers locations were compared against the equivalent barriers locations based on the high-resolution (1 m x 1 m) DTM and show a higher degree of agreement for water harvesting structures longer in length. The implication is that using a high-resolution DEM will give more accurate results. That said, SiteFinder is intended for use in scoping, so all potential sites will require detailed, ground-based survey at a later stage. The risk however, especially when using a 1 arc-second DSM as here, is that when identifying smaller water harvesting structures (e.g., Scenarios 2 and 3), selected sites may have quite different parameters than those predicted by the tool and possibly some locations that would make suitable sites for water harvesting structures are missed.

SiteFinder calculates the barrier crest width as being fixed at just 0.25 m. This is somewhat less than the 3 m proposed by Nissen-Petersen (2006), so the tool could be used for low standing water harvesting structures without significantly overestimating the barrier volume. A future refinement of the tool could set the crest width as a function of the height of the barrier (Stephens, 2010) as well as allowing the user more control over the design of the barrier structure to match the water harvesting technique.

For the three scenarios presented in the case study, SiteFinder was only used to find potential locations for water harvesting structures. In the locations identified, runoff from the outer limits of the catchment area would need to flow some distance before reaching the area of influence where it would be impounded (Fig. 5, Fig. 6, Fig. 7). No analysis was undertaken to test the functionality of the SiteFinder in finding sites suitable for in-situ water harvesting. GIS-based decision support systems have been used to identify areas suitable for in-situ water harvesting (Mahmoud and Alazba, 2015) and this is a potential further application of the tool. A feature of SiteFinder is that the barrier axis is set perpendicular to the flow direction, calculated using the D8 procedure, described by Jenson and Domingue (1988). This D8 flow direction is also the basis for siting point identification since the flow accumulation raster is created with the D8 flow direction raster as the input. Other flow direction methods do exist such as multi-flow-direction (MFD) (Qin et al., 2007) and D-Infinity (Tarboton, 1997). Future research could

investigate if these flow direction methods would be preferable to the D8 method in setting the barrier axis direction. Similarly, it would be interesting to determine if some flow direction methods offer advantages to others for siting point identification, especially if SiteFinder is to be used for both external and in-situ water harvesting. Orlandini and Moretti (2009) concluded that the choice of using non-dispersive methods over dispersive methods is dependent on the need to delineate flow paths or to focus on divergent terrains. This tentatively suggests that dispersive flow direction methods would be more applicable for in-situ water harvesting and non-dispersive methods (e.g., D8) better for external water harvesting.

None of the filtered barriers (Table 2, Table 3, Table 4) are presented as recommendations for water harvesting sites since some criteria typically incorporated into a site selection process were not considered. SiteFinder does however demonstrate its capacity to generate pertinent site characteristics within a GIS environment that could form part of a multi-criteria approach (MCA) to water harvesting site identification. Therefore, a future development would be to use SiteFinder as part of a 'real-world' MCA water harvesting site selection process considering a range of biophysical, socio-economic, and environmental criteria, with the aim of identifying suitable locations prior to any site visit.

## 5. Conclusions

A novel methodology has been presented for automatically obtaining the characteristics of potential external water harvesting sites using a script-based tool operating entirely within a GIS environment using a digital elevation product as the primary source of information. Using an automated process, a total of 5,770 sites were analysed, the characteristics of barriers computed, resulting in the selection of sites based on water harvesting site selection parameters. To our knowledge, this is the first time that details of potential sites, including details of the barrier (height, length and volume) and storage geometry, have been automatically calculated within a GIS environment. Outputs are provided in geospatial formats including barriers represented by lines, and polygons representing the area of influence linked to each barrier. The tool functions using low-to-high resolution elevation datasets and can find site characteristics for any size water harvesting structure.

Since GIS is used extensively by researchers as part of water harvesting site selection processes it is envisaged that SiteFinder could be readily assimilated into decision-making methods, enabling combination of outputs created by this tool with other biophysical, socio-economic, and environmental criteria to aid the identification of potential water harvesting sites.

It is suggested that SiteFinder is best suited for scoping, prior to any field-visits, automatically calculating the catchment area, storage capacity, and barrier dimensions for potential ex-situ water harvesting earth embankments with a 0.25 m crest width and fixed slope but with future refinements the tool could offer greater control over the barrier specifications (e.g., shape, slope, and crest width) allowing a wider range of water harvesting structures to be analysed. It is recommended that further research is undertaken to ascertain the quality of the digital elevation products (e.g., in relation to spatial resolution and vertical accuracy) required to compute the geometry of potential water harvesting structures to within acceptable levels of uncertainty.

## Declaration of Competing Interest

The authors declare that they have no known competing financial interests or personal relationships that could have appeared to influence the work reported in this paper.

## Data Availability

The authors do not have permission to share data.

## Acknowledgements

We thank United Nations Office for Project Services (UNOPS) Sudan for their kind permission to use survey data of Tawila Dam (North Darfur, Sudan). We also thank the user support staff at CEDA (<https://www.ceda.ac.uk/about>) and JASMIN (<https://www.jasmin.ac.uk/about/>) for their help in accessing and use of their computer facilities and similarly we thank the help desk staff at the NERC Earth Observation Data Acquisition and Analysis Service (NEODAAS) (<https://nerc-arf-dan.pml.ac.uk/>) desk for support in obtaining and processing the airborne survey data. We also thank the two anonymous reviewers of this paper for their constructive comments.

## Appendix A. Supporting information

Supplementary data associated with this article can be found in the online version at [doi:10.1016/j.agwat.2022.107836](https://doi.org/10.1016/j.agwat.2022.107836).

## References

- Abdalla, O.A.E., Al-Rawahi, A.S., 2013. Groundwater recharge dams in arid areas as tools for aquifer replenishment and mitigating seawater intrusion: example of AlKhod, Oman. *Environ. Earth Sci.* <https://doi.org/10.1007/s12665-012-2028-x>.
- Abdullah, M., Al-Ansari, N., Laue, J., 2020. Water harvesting in Iraq: status and opportunities. *J. Earth Sci. Geotech. Eng.* 10, 1792–9660.
- Adham, A., Riksen, M., Ouessar, M., Coen, R., 2016. Identification of suitable sites for rainwater harvesting structures in arid and semi-arid regions: a review. *Int. Soil Water Conserv. Res.* 4, 108–120. <https://doi.org/10.1016/j.iswcr.2016.03.001>.
- Adham, A., Wesseling, J.G., Abed, R., Riksen, M., Ouessar, M., Ritsema, C.J., 2019. Assessing the impact of climate change on rainwater harvesting in the Oum Zessar watershed in Southeastern Tunisia. *Agric. Water Manag.* 221, 131–140. <https://doi.org/10.1016/j.agwat.2019.05.006>.
- Agriculture Victoria, 2020. Drought Reserve Dams [WWW Document]. Agric. Victoria. URL <https://agriculture.vic.gov.au/farm-management/water/managing-dams/drought-reserve-dams> (accessed 3.24.22).
- Airborne Research and Survey Facility (2009): Data from the Photographic Camera, Optech LIDAR and AISA Eagle and Hawk Instruments on-board the Dornier Do228-101 D-CALM Aircraft during Flight ET07/03 over the Alem Tena Area, Ethiopia. NERC Earth Observation Data Centre, (7.30.20). <https://catalogue.ceda.ac.uk/uuid/b30490c666dd23b43789412183602a5c>.
- Al-Adamat, R., 2008. GIS as a decision support system for siting water harvesting ponds in the basalt aquifer/NE Jordan. *J. Environ. Assess. Policy Manag.* 10, 189–206. <https://doi.org/10.1142/S146433208003020>.
- Al-Khuzai, M.M., Janna, H., Al-Ansari, N., 2020. Assessment model of water harvesting and storage location using GIS and remote sensing in Al-Qadisiyah, Iraq. *Arab. J. Geosci.* 13, 1–9. <https://doi.org/10.1007/s12517-020-06154-4>.
- American Water Works Association, 2006. *Water Chlorination/Chloramination Practices and Principles - Manual of Water Supply Practices, M20, 2nd Edition*. American Water Works Association, Denver, Colo.
- Banai-Kashani, R., 1989. A new method for site suitability analysis: the analytic hierarchy process. *Environ. Manag.* 13, 685–693. <https://doi.org/10.1007/BF01868308>.
- Binnie, C., Kimber, M., Thomas, H., 2018. *Basic Water Treatment, sixth ed.* ICE Publishing, London.
- Boers, T.M., Ben-Asher, J., 1982. A review of rainwater harvesting. *Agric. Water Manag.* 5, 145–158. [https://doi.org/10.1016/0378-3774\(82\)90003-8](https://doi.org/10.1016/0378-3774(82)90003-8).
- Boers, T.M., 1994. Rainwater Harvest. Arid semi-Arid zones. *Int. Inst. Land Reclam.*
- Bruins, H.J., Evenari, M., Nessler, U., 1986. Rainwater-harvesting agriculture for food production in arid zones: the challenge of the African famine. *Appl. Geogr.* 6, 13–32. [https://doi.org/10.1016/0143-6228\(86\)90026-3](https://doi.org/10.1016/0143-6228(86)90026-3).
- Caincross, S., Feachem, R.G., 1993. *Environmental health engineering in the tropics: an introductory text, 2nd ed.* J. Wiley, Chichester.
- Critchley, W., Siegert, K., 1991. *A Manual for the design and construction of water harvesting schemes for plant production*. Food and Agriculture Organisation of the United Nations, Rome, Italy. Food and Agriculture Organization of The United Nations, Rome, Italy.
- Earth Resources Observation and Science (EROS) Center, 2018a. USGS EROS archive - digital elevation - shuttle radar topography mission (SRTM) 1 arc-second global [WWW Document] Usgs. URL, doi: 10.5066/F7PR7TFT.accessed 11.18.20.
- Earth Resources Observation and Science (EROS) Center, 2018b. USGS EROS archive - digital elevation - shuttle radar topography mission (SRTM) void filled [WWW Document] Usgs. URL 2018b doi: 10.5066/F7F76B1X.accessed 11.15.20.
- Ettazarini, S., 2021. GIS-based land suitability assessment for check dam site location, using topography and drainage information: a case study from Morocco. *Environ. Earth Sci.* 80. <https://doi.org/10.1007/s12665-021-09881-3>.
- Falorni, G., Teles, V., Vivoni, E.R., Bras, R.L., Amaratunga, K.S., 2005. Analysis and characterization of the vertical accuracy of digital elevation models from the Shuttle Radar Topography Mission, 110, FO2005-n/a *J. Geophys. Res. Earth Surf.* <https://doi.org/10.1029/2003JF000113>.
- Farswan, S., Vishwakarma, C.A., Mina, U., Kumar, V., Mukherjee, S., 2019. Assessment of rainwater harvesting sites in a part of North-West Delhi, India using geomatic tools. *Environ. Earth Sci.* 78. <https://doi.org/10.1007/s12665-019-8332-y>.
- Forzieri, G., Gardenti, M., Caparrini, F., Castelli, F., 2008. A methodology for the pre-selection of suitable sites for surface and underground small dams in arid areas: A case study in the region of Kidal, Mali. *Phys. Chem. Earth* 33, 74–85. <https://doi.org/10.1016/j.pce.2007.04.014>.
- Gallant, J.C., Read, A.M., Dowling, T.I., 2012. Removal of tree offsets from SRTM and other digital surface models. *Int. Arch. Photogramm. Remote Sens. Spat. Inf. Sci.* <https://doi.org/10.5194/isprsarchives-xxxix-b4-275-2012>.
- Geyik, M.P., 1986. *FAO Watershed Manag. Field Man. Gully Control* FAO Conserv. Guide 13/2.
- Haile, G., Suryabhagavan, K.V., 2019. GIS-based approach for identification of potential rainwater harvesting sites in Arsi Zone, Central Ethiopia. *Model. Earth Syst. Environ.* 5, 353–367. <https://doi.org/10.1007/s40808-018-0537-7>.
- Helmreich, B., Horn, H., 2009. Opportunities in rainwater harvesting. *Desalination* 248, 118–124. <https://doi.org/10.1016/j.desal.2008.05.046>.
- International Commission on Large Dams / Commission Internationale des Barrages, (ICOLD/CIGB), 2011. Constitution Statuts [WWW Document]. URL [https://www.icold-cigb.org/userfiles/files/CIGB/INSTITUTIONAL\\_FILES/Constitution2011.pdf](https://www.icold-cigb.org/userfiles/files/CIGB/INSTITUTIONAL_FILES/Constitution2011.pdf) (accessed 8.9.21).
- Jenson, S.K., Domingue, J.O., 1988. Extracting topographic structure from digital elevation data for geographic information system analysis. *Photogramm. Eng. Remote Sens.* 54, 1593–1600.
- Jothiprakash, V., Sathe, M.V., 2009. Evaluation of rainwater harvesting methods and structures using analytical hierarchy process for a large scale industrial area. *J. Water Resour. Prot.* 01, 427–438. <https://doi.org/10.4236/jwarp.2009.16052>.
- Kadam, A.K., Kale, S.S., Pande, N.N., Pawar, N.J., Sankhua, R.N., 2012. Identifying potential rainwater harvesting sites of a semi-arid, basaltic region of Western India, Using SC5-CN method. *Water Resour. Manag.* 26, 2537–2554. <https://doi.org/10.1007/s11269-012-0031-3>.
- Karnieli, A., Ben-Asher, J., Dodi, A., Issar, A., Oron, G., 1988. An empirical approach for predicting runoff yield under desert conditions. *Agric. Water Manag.* 14, 243–252. [https://doi.org/10.1016/0378-3774\(88\)90078-9](https://doi.org/10.1016/0378-3774(88)90078-9).
- Krois, J., Schulte, A., 2014. GIS-based multi-criteria evaluation to identify potential sites for soil and water conservation techniques in the Ronquillo watershed, northern Peru. *Appl. Geogr.* 51, 131–142. <https://doi.org/10.1016/j.apgeog.2014.04.006>.
- Li, L., Yang, J.S., Sun, W.Y., Shen, S.S., 2018. Analysis of the typical small watershed of warping dams in the sand properties. *E3S Web Conf.* 38, 03052. <https://doi.org/10.1051/e3sconf/20183803052>.
- Logsdon, G.S., 2008. Water filtration practices including slow sand filters and precoat filtration, 1st ed. American Water Works Association, Denver, Colo.
- Mahmoud, S.H., Alazba, A.A., 2015. The potential of in situ rainwater harvesting in arid regions: developing a methodology to identify suitable areas using GIS-based decision support system. *Arab. J. Geosci.* 8, 5167–5179. <https://doi.org/10.1007/s12517-014-1535-3>.
- Mati, B., Bock, T. De, Bancy Mati, Bock, Tanguy De, Malesu, M., Khaka, E., Oduor, A., Nyabenge, M., Oduor, V., 2006. Mapping the Potential of Rainwater Harvesting Technologies in Africa: A GIS overview on development domains for the continent and ten selected countries, Technical Manual No. 6. World Agroforestry Centre (ICRAF), Netherlands Ministry of Foreign Affairs, Nairobi, Kenya.
- Mekdaschi, R., Liniger, H., 2013. *Water harvesting: guidelines to good practice*. Centre for Development and Environment.
- Mohammed, H.M.H., 2018. Topographic Survey of Tawila Dam, North Darfur State, Sudan [unpublished raw dataset]. Practical Consultancy Engineering Co. Ltd. Khartoum.
- Mugo, G.M., Odera, P.A., 2019. Site selection for rainwater harvesting structures in Kiambu County-Kenya. *Egypt. J. Remote Sens. Space Sci.* 22, 155–164. <https://doi.org/10.1016/j.ejrs.2018.05.003>.
- Niemeijer, D., 1998. Soil nutrient harvesting in indigenous Teras water harvesting in eastern Sudan. *L. Degrad. Dev.* 9, 323–330. [https://doi.org/10.1002/\(SICI\)1099-145X\(199807/08\)9:4<323::AID-LDR295>3.0.CO;2-N](https://doi.org/10.1002/(SICI)1099-145X(199807/08)9:4<323::AID-LDR295>3.0.CO;2-N).
- Nissen-Petersen, E., 2006. *Water from Small Dams A handbook for technicians, farmers and others on site investigations, designs, cost estimates, construction and maintenance of small earth dams*. ASAL Consultants Ltd. for the Danish International Development Assistance (Danida) in Kenya.
- OpenTopography, 2008. *OpenTopography High-Resolution Topography Data and Tools* [WWW Document]. OpenTopography. URL [https://portal.opentopography.org/data\\_sets](https://portal.opentopography.org/data_sets) (accessed 9.3.19).
- Orlandini, S., Moretti, G., 2009. Determination of surface flow paths from gridded elevation data. *Water Resour. Res.* 45. <https://doi.org/10.1029/2008WR007099>.
- Padmavathy, A.S., Ganesha Raj, K., Yogarajan, N., Thangavel, P., Chandrasekhar, M.G., 1993. Checkdam site selection using GIS approach. *Adv. Sp. Res.* 13, 123–127. [https://doi.org/10.1016/0273-1177\(93\)90213-U](https://doi.org/10.1016/0273-1177(93)90213-U).
- Panagopoulos, A., 2021. Water-energy nexus: desalination technologies and renewable energy sources. *Environ. Sci. Pollut. Res. Int.* 28, 21009–21022. <https://doi.org/10.1007/s11356-021-13332-8>.
- Papenfus, N., 2003. *Criteria for Siting Dams* [WWW Document]. Dams Africa. URL <http://www.damsforafrica.com/investigations-reports-proposals.html> (accessed 3.24.22).
- Petheram, C., Gallant, J., Read, A., 2017. An automated and rapid method for identifying dam wall locations and estimating reservoir yield over large areas. *Environ. Model. Softw.* 92, 189–201. <https://doi.org/10.1016/j.envsoft.2017.02.016>.
- Piemontese, L., Castelli, G., Fetzer, H., Barron, J., Liniger, H., Harari, N., Bresci, E., Jaramillo, F., 2020. Estimating the global potential of water harvesting from

- successful case studies. *Glob. Environ. Chang* 63, 102121. <https://doi.org/10.1016/j.gloenvcha.2020.102121>.
- Qin, C., Zhu, A.X., Pei, T., Li, B., Zhou, C., Yang, L., 2007. An adaptive approach to selecting a flow-partition exponent for a multiple-flow-direction algorithm. *Int. J. Geogr. Inf. Sci.* 21, 443–458. <https://doi.org/10.1080/13658810601073240>.
- Reseigh, J., 2021. Controlling Dam Evaporation [WWW Document]. Sheep Connect South Aust. URL <https://www.sheepconnectsa.com.au/management/water/dams/controlling-dam-evaporation> (accessed 7.2.21).
- Rockström, J., Falkenmark, M., 2015. Agriculture: increase water harvesting in Africa. *Nature* 519, 283–285. <https://doi.org/10.1038/519283a>.
- Salih, S.A., Al-Tarif, A.S.M., 2012. Using of GIS spatial analyses to study the selected location for dam reservoir on Wadi Al-Jirnaf, West of Shirqat Area, Iraq. *J. Geogr. Inf. Syst.* 04, 117–127. <https://doi.org/10.4236/jgis.2012.42016>.
- Sayl, K.N., Muhammad, N.S., El-Shafie, A., 2019. Identification of potential sites for runoff water harvesting. *Proc. Inst. Civ. Eng. Water Manag.* 172, 135–148. <https://doi.org/10.1680/jwama.16.00109>.
- Schumann, G.J.-P., Bates, P.D., 2018. The need for a high-accuracy, open-access global DEM. *Front. Earth Sci.* 6, 225. <https://doi.org/10.3389/feart.2018.00225>.
- Sekar, I., Randhir, T.O., 2007. Spatial assessment of conjunctive water harvesting potential in watershed systems. *J. Hydrol.* 334, 39–52. <https://doi.org/10.1016/j.jhydrol.2006.09.024>.
- Şen, Z., Al Alsheikh, A., Al-Turbak, A.S., Al-Bassam, A.M., Al-Dakheel, A.M., 2013. Climate change impact and runoff harvesting in arid regions. *Arab. J. Geosci.* 6, 287–295. <https://doi.org/10.1007/s12517-011-0354-z>.
- Siabi, W.K., 2008. Access to Sanitation and Safe Water: Aeration and its application in groundwater purification, in: 33rd WEDC International Conference, Accra, Ghana, 2008. 33rd WEDC International Conference, Accra, Ghana, 2008, Ghana.
- Stephens, T., 2010. Manual on small earth dams, A guide to siting, design and construction, FAO drainage and irrigation paper, Number 64. Food & Agriculture Organisation of the United Nations, Rome, Italy.
- Strahler, A.N., 1957. Quantitative analysis of watershed geomorphology. *Eos Trans. Am. Geophys. Union* 38, 913–920. <https://doi.org/10.1029/TR038i006p00913>.
- Tarboton, D.G., 1997. A new method for the determination of flow directions and upslope areas in grid digital elevation models. *Water Resour. Res.* 33, 309–319. <https://doi.org/10.1029/96WR03137>.
- Teschemacher, S., Bittner, D., Disse, M., 2020. Automated location detection of retention and detention basins for water management. *Water* 12, 1491. <https://doi.org/10.3390/w12051491>.
- United States Department of Agriculture (USDA), 1997. Ponds — Planning, Design, Construction, Agriculture Handbook Number 590. US Department of Agriculture.
- V.M. Castillo, V.M., Mosch, W.M., García, C.C., Barberá, G.G., Cano, J.A.N., López-Bermúdez, F., 2007. Effectiveness and geomorphological impacts of check dams for soil erosion control in a semiarid Mediterranean catchment: El Cárcavo (Murcia, Spain Catena (Giess.)), 70, pp. 416–427 doi: [10.1016/j.catena.2006.11.009](https://doi.org/10.1016/j.catena.2006.11.009).
- Van Dijk, J.A., Ahmed, M.H., 1993. Opportunities for expanding water harvesting in Sub-Saharan Africa: the case of the Teras of Kassala, Opportunities for Expanding Water Harvesting in Sub-Saharan Africa. International Institute for Environment and Development.
- Tumbo, S.D., Mbilinyi, B.P., Mahoo, H.F., Mkilamwinyi, F.O., 2014. Identification of suitable indices for identification of potential sites for rainwater harvesting. *Tanzania J. Agric. Sci.* 12, 35–46.
- Vema, V., Sudheer, K.P., Chaubey, I., 2019. Fuzzy inference system for site suitability evaluation of water harvesting structures in rainfed regions. *Agric. Water Manag* 218, 82–93. <https://doi.org/10.1016/j.agwat.2019.03.028>.
- Wang, Q., Zhang, E., Li, Fengmin, Li, Fengrui, 2008. Runoff efficiency and the technique of micro-water harvesting with ridges and furrows, for potato production in semi-arid areas. *Water Resour. Manag.* 22, 1431–1443. <https://doi.org/10.1007/s11269-007-9235-3>.
- Wang, Y., Tian, Y., Cao, Y., 2021. Dam siting: a review. *Water* 13, 2080. <https://doi.org/10.3390/w13152080>.
- Wimmer, M.H., Pfeifer, N., Hollaus, M., 2019. Automatic detection of potential dam locations in digital terrain models. *ISPRS Int. J. Geo-Inf.* 8, 197. <https://doi.org/10.3390/ijgi8040197>.
- de Winnaar, G., Jewitt, G.P.W., Horan, M., 2007. A GIS-based approach for identifying potential runoff harvesting sites in the Thukela River basin, South Africa. *Phys. Chem. Earth* 32, 1058–1067. <https://doi.org/10.1016/j.pce.2007.07.009>.
- Zaidi, F.K., Nazzal, Y., Ahmed, I., Naeem, M., Jafri, M.K., 2015. Identification of potential artificial groundwater recharge zones in Northwestern Saudi Arabia using GIS and Boolean logic. *J. Afr. Earth Sci.* 111, 156–169. <https://doi.org/10.1016/j.jafrearsci.2015.07.008>.
- Ziadat, F., Bruggeman, A., Oweis, T., Haddad, N., Mazahreh, S., Sartawi, W., Syuof, M., 2012. A participatory GIS approach for assessing land suitability for rainwater harvesting in an arid rangeland environment. *Arid Land Res. Manag.* 26, 297–311. <https://doi.org/10.1080/15324982.2012.709214>.
- Zumrawi, M., 2015. Failure investigation of Tawila Dam in North Darfur. *Sudan Int. J. Sci. Res.* 438, 963–967.